Research Article

Tianyu Jiang, Naeem ul Haq Tariq, Xiang Qiu, Qichao Zhang*, Lin Li*, and Jialun Du*

An effective approach to improve microstructure and tribological properties of cold sprayed Al alloys

https://doi.org/10.1515/rams-2023-0314
received October 26, 2022; accepted April 12, 2023

Abstract: Cold spray is considered as an emerging technique for preparing wear-resistant metal matrix composite coatings on the surface of various kinds of metallic materials. In this work, a viable strategy of "cold spraying + hot rolling post-treatment" was successfully applied to prepare wear-resistant B_4C/6061 Al composite coating on commercially available 6061 Al plates. The results revealed that hot rolling post-treatment results in uniform distribution of B_4C particles in the alloy matrix, good inter-splat bonding, and sufficient plasticity in the splats through effective healing of the defects and splat boundaries in the as-sprayed deposit. As a result, the coating/substrate bonding strength in the hot rolled sample increased two-fold when compared with that of the as-sprayed sample. Moreover, hot rolling process resulted in much improved tribological properties of the coating with the wear rate ~40% of that of the substrate. The obtained results indicated that the idea of combining cold spraying and hot rolling treatment is quite effective for improving the tribological properties of Al alloy plates. Further, this approach seems equally good for repairing/remanufacturing of unserviceable 6061 Al alloy components.

*** Corresponding author: Qichao Zhang,** Navy Submarine Academy, Qingdao 260199, China; CAS Key Laboratory of Marine Environment of Corrosion and Bio-fouling, Institute of Oceanology, Chinese Academy of Sciences, Qingdao 266071, China, e-mail: zhangqcocean@163.com
*** Corresponding author: Lin Li,** Department of Petroleum Engineering, China University of Petroleum (East China), Qingdao 266580, China, e-mail: lilin@upc.edu.cn
*** Corresponding author: Jialun Du,** Yantai University, Yantai 264005, China, e-mail: 69300569@qq.com
Tianyu Jiang: Department of Petroleum Engineering, China University of Petroleum (East China), Qingdao 266580, China
Naeem ul Haq Tariq: Department of Metallurgy and Materials Engineering, Pakistan Institute of Engineering and Applied Sciences, Nilore, Islamabad, Pakistan
Xiang Qiu: Institute of Metal Research, Chinese Academy of Sciences, Shenyang 110016, China

Keywords: B_4C/6061 Al, cold spray, bonding strength, tribological properties

1 Introduction

Cold spray (CS) is an emerging solid-state coating and additive manufacturing technique for variety of metals, alloys and composites [1]. During CS process, micro-scale feedstock powders are accelerated by a converging-diverging (de Laval) type nozzle to form a supersonic jet which is then impacted on the substrate surface to form a coating layer by layer through severe plastic deformation of the metallic particles [2,3]. Because of the extremely short time of particle deposition (less than 10^{-6} s), it is difficult to fully understand the *in situ* deposition process through experimental methods. Therefore, at present, the study of particle deposition mechanism and impact phenomena are generally studied by simulations. For example, Viscusi *et al.* proposed a computational fluid dynamics model focusing on both geometrical features and spray behavior and found that the deposition efficiency tends to decrease due to the critical phenomena occurring in the spray nozzle during long time depositions [4]. Moreover, they developed 3D FEM model for cold spray process to simulate the particle/substrate bonding phenomena. Further, they found an effective window for deposition, which could be extended by increasing the contact area thus further increasing the cold spray deposition efficiency [5].

Thanks to its low processing temperature, oxidation, phase transformation and residual thermal stresses (which are usually encountered in the conventional high-temperature spraying processes) can be effectively avoided in CS process [6–8]. Therefore, CS is technically available to deposit a variety of functional coatings such as metals, metal matrix composites and even ceramics with the thickness ranging from micron to millimeter or even decimeter scale [9]. Particularly, CS shows incomparable advantage in fabricating Al-based materials because of its comprehensive

characteristics of low melting point, good deformability, easy deposition and high reflectivity [10,11].

To date, a large number of studies have been carried out to improve the wear-resistance of Al-based coatings by introducing ceramic particles (*i.e.*, B_4C [12], SiC [13], Al_2O_3 [2] and BN [14]) in the feedstock powder to prepare composite coatings. Generally, it is believed that the ceramic particles act as load bearing phase during sliding process thereby resulting in significant reduction in wear loss of the coating through third-body effect [15]. Despite the abovementioned advantages, preparation of Al-based composites by CS still remains a challenging job, since ceramic and metallic particles in the cold sprayed coating remain in simple physical contact without any interfacial reaction. Therefore, abrasion resistance of the composite coatings remains below par due to poor ceramic/metallic interface bonding [16]. Further, sharp-angle morphology of ceramic particles makes it easy to be embedded in the substrate during the spraying process. This results in the formation of discontinuous isolation zone at coating/substrate interface which significantly reduces coating/substrate interface bonding. As a result, the composite coatings can be easily peeled off from the surface of substrate under the action of external force [17]. Therefore, it is of prime importance to improve the deposition behavior of ceramic particles (in cold sprayed composite coatings) to achieve good ceramic/metallic interface bonding.

In this context, researchers have made few attempts to improve the wear resistance by altering the microstructure of cold sprayed coatings. For example, Siddique *et al.* showed that heat treatment can improve splat-splat interface bonding, thus theoretically improving the wear resistance of the coating [18]. However, it is reported that although particle delamination phenomenon is significantly reduced in the heat treated coatings during friction process, yet softening of the heat treated coating results in severe ploughing, which ultimately increases the wear loss [19]. Therefore, under the effect of these two competitive factors, wear resistance of the heat treated composite coatings could not be greatly improved [19,20]. Quite recently, a method of densifying the coating (by adding hard and large sized spherical particles into the original powder) has been reported [21,22]. This approach resulted in high quality dense coatings due to *in situ* micro-forging effect of hard and large sized spherical particles. Theoretically, *in situ* micro-forging remarkably decreases the porosity and greatly improves splat-splat interfacial bonding in all type of cold sprayed coatings. According to the previous research [23,24], although the tribological properties of the coating (prepared by this method) were improved, the ceramic particles in the coating were fragmented due to severe impact of the large sized hard particles, thus resulting in the formations of internal cracks in the prepared coating. Moreover, the large sized hard particles inevitably remained in the coating. To address this issue, Chen *et al.* recently proposed the use of core-shell structured composite powders (composed of a ductile metal shell and a hard core) in the feedstock. During CS operation, the metallic shell experienced severe plastic deformation upon impact with the substrate or previously deposited material, thus resulting in a good metallurgical bonding [10]. Consequently, the prepared coating exhibited superior wear resistance. However, the use of such core-shell powders seems to be cost-prohibited when employed in the industry for mass scale production.

Recently, we reported a unique way to fabricate Ti/steel clad plate by cold spraying Ti powder on steel substrate and subsequent hot rolling co-treatment. The obtained composite sheet exhibited high compaction, uniform microstructure and high coating/substrate adhesion strength [25,26]. Moreover, the fundamental aspects of the freestanding cold sprayed + hot rolled Al alloy material was examined in detail in a different study [27]. Our results demonstrated that hot rolling process not only efficiently improves splat-splat bonding but also results in progressive refinement and uniform distribution of the reinforcement in α-Al matrix [27].

Based on these findings, here we propose a new strategy for preparing high wear-resistant composite coating using a combination of cold spraying and hot rolling. To the authors' knowledge, there is no previous study demonstrating the improvement of surface wear resistance of Al alloy using this unique processing combination. In this study, 6061 Al/B_4C composite coating was successfully deposited on commercial grade 6061 Al alloy by cold spraying followed by hot rolling. The microstructure and tribological properties of the prepared coating, under different processing conditions, are studied in detail. Since 6061 Al alloy is the most commonly used structural material in automobile and aerospace industry (owing to its low processing cost, excellent mechanical and corrosion properties) [28] and the alloy products are often degraded under harsh service environment, therefore, it was selected as the substrate material to enhance its wear resistance. Further, the possibility of repairing/remanufacturing of unserviceable 6061 Al alloy parts was also explored.

2 Materials and methods

Figure 1 shows a schematic diagram of the main experimental procedures including cold spray process, post-treatments and performance tests for the composite coatings. The specific detail of each of the process is as follows.

2.1 Sample preparation

In this study, a commercially available 6061 Al plate with dimensions of 100 × 100 × 3 mm^3 was selected as the substrate while gas atomized 6061 Al alloy powder and irregular shaped B_4C powder were used as the feedstock powder for cold spraying process. The as-received powders were mixed together with the formulation of 70 wt% 6061 Al and 30 wt% B_4C and were mechanically blended in a rotary mill at a speed of 150 rpm for 8 h. After blending process, feedstock powders were vacuum packed for subsequent cold spraying experiment. CS was performed using a commercial medium/high pressure IMR-600 CS device equipped with a rectangular de Laval type nozzle. Details of this CS system can be found elsewhere [27]. The distance from the throat (having a diameter of 2.5 mm) to the exit (having a diameter of 7.1 mm) of the nozzle was 58.5 mm. Prior to CS process, the 6061 Al alloy substrate was sand-blasted using 120 grit SiO_2 sand to keep the surface clean and free from oxidation. During CS process, compressed air was used as the carrier gas with the temperature and pressure of 350°C and 3 MPa, respectively. The nozzle was moved on the substrate at a line speed of 5 mm·s^{-1} and the stand-off distance of 10 mm. Powder feed rate was set to 25 ± 5 g·min^{-1} throughout the deposition process. The final thickness of the coating was ~1.5 mm. After CS process, heat treatment and hot rolling post-processes were carried out to improve the microstructure of the prepared coating. For heat treatment, samples were placed in a vacuum muffle oven at 350°C for 4 h followed by cooling in the furnace. For hot rolling, samples with dimensions of 20 × 40 × 3.5 mm^3 were sectioned and heated at 500°C for 2 h in a furnace. Subsequently, rolling process was performed at a rolling speed of 0.3 mm·s^{-1} and a thickness reduction of 20% was achieved in 1 pass.

2.2 Materials characterization

Scanning electron microscopy (SEM; Zeiss Merlin Compact, Germany) was used to examine the morphology of the feedstock powder and the microstructure evolution in the prepared coatings at different processing stages. In order to observe the cross-sectional microstructure, samples were prepared according to the standard metallographic procedures. X-ray diffraction (XRD) analysis of different coatings was carried out using a X'Pert MPD diffractometer (Philips, Holland) with a scanning rate of 0.02°·s^{-1} (Cu Kα radiation). Microhardness measurements were performed at the middle region of the cross-section of the coating using a Vickers Microhardness Tester (Leco AMH43, USA). For each

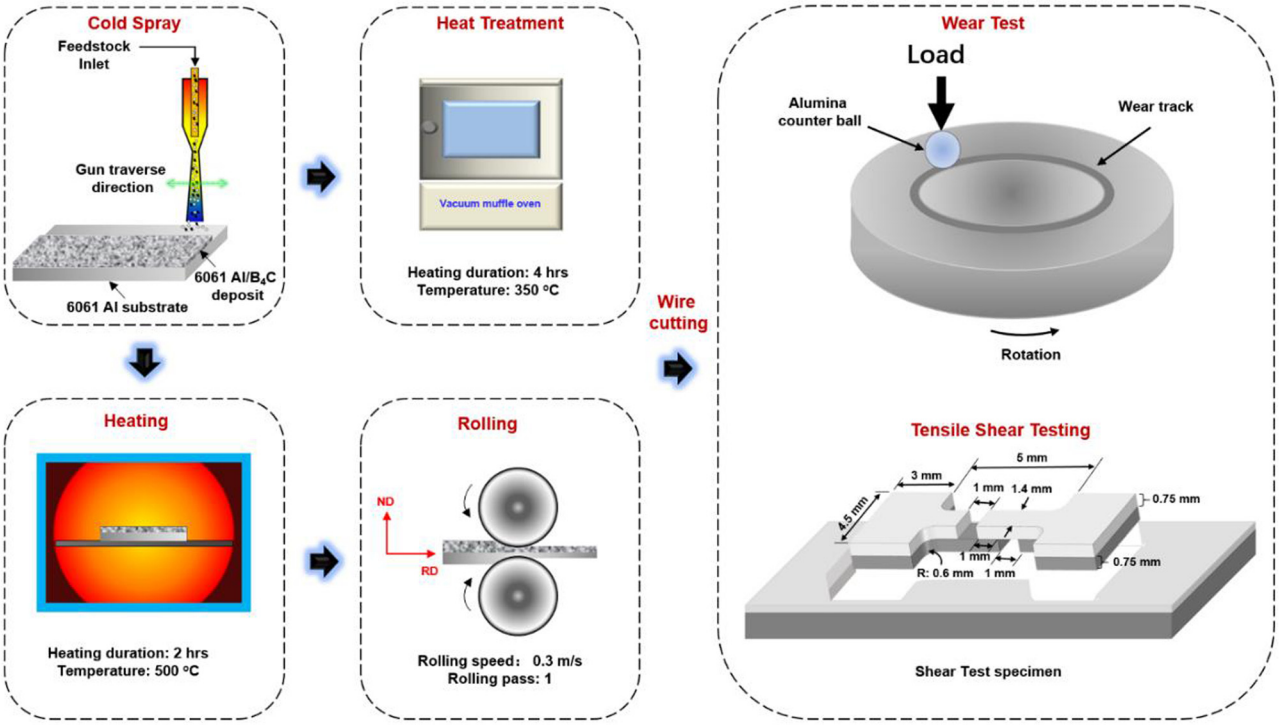

Figure 1: Schematic diagram summarizing all experimental procedures for the composite coatings.

sample, at least 15 equally spaced indentations were made using a load of 300 gf and a holding time of 15 s. In order to investigate the bonding strength of the coatings, a series of shear tests were conducted in accordance with ISO 6892-1:2009 standard. The dimensions of the shear test samples are shown in Figure 1. An electronic dynamic and static universal testing machine (INSTRON 5848, UK) was used to perform the shear test at a strain rate of 10^{-3} s^{-1}. After performing shear tests, SEM was used to study the fractured surface of the samples.

2.3 Wear test

Room temperature sliding wear tests were carried out with a ball-on-disc system. Prior to the wear test, samples were ground by 200–2000# sandpapers followed by polishing using 0.5 µm diamond suspension. An alumina ball, with a diameter of 4 mm, was selected as the counter material in this test. A normal load of 3 N was applied on the counter ball. During wear test, samples were fixed on the holder and rotated in a diameter of 6 mm with a speed of 200 rpm. This resulted in the formation of a circular wear track with a diameter of 6 mm. After wear test for a duration of 30 min, the total wear length was around 113 m. The friction force and the friction coefficient were dynamically recorded by a computer program. The cross-sectional area of the wear track was determined by a surface profilometer (Alpha-Step IQ, KLA, USA). For this purpose, at least 12 different randomly selected areas of the worn trace were selected to ensure the accuracy of the results. Finally, wear surface topography was analyzed by SEM and a non-contact surface mapping microscope (3D Micro XAM, KLA, USA).

3 Results and discussion

Figure 2 shows SEM image of the as-mixed B_4C/6061 Al feedstock powders. It can be observed that both powders are uniformly mixed with each other. The 6061 Al powder maintains its spherical morphology after blending with average size of ~20 µm. The B_4C particles exhibit angular morphology with average particle size of ~5 µm. The magnified SEM image in Figure 2(b) shows that some fine B_4C particles (as marked by red arrow in Figure 2(b)) have achieved good pre-bonding thereby sticking with the surface of 6061 Al powder after mixing operation.

Figure 3 shows SEM backscattered cross-sectional images of as-sprayed, heat-treated and hot-rolled samples at different magnifications. It can be observed that all the coatings have relatively dense structure, indicating sufficient plastic deformation of 6061 Al particles during the spraying process. However, the microstructures of these three samples were quite different. In case of as-sprayed sample, the content of B_4C particles in the coating (9.30 ± 0.07 vol%) is significantly lower than those of the heat treated (18.55 ± 0.39 vol%) and hot rolled samples (13.58 ± 0.05 vol%). This is attributed to the high degree of work hardening and the resulting brittleness of the material. During the process of mechanical grinding/polishing, the degree of adaptive plastic flow between the matrix and the ceramic particles was poor, thus resulting in the pulling off some B_4C particles along with the formation of few voids (as highlighted by the yellow arrow in Figure 3(c)). Similar results were also reported by Tariq *et. al* for cold sprayed Al-B_4C composite coating [28]. Moreover, it can be observed that B_4C particles are generally distributed along the boundary of deformed 6061 Al particles, as marked by the red virtual line in Figure 3(c). This may lead to the local

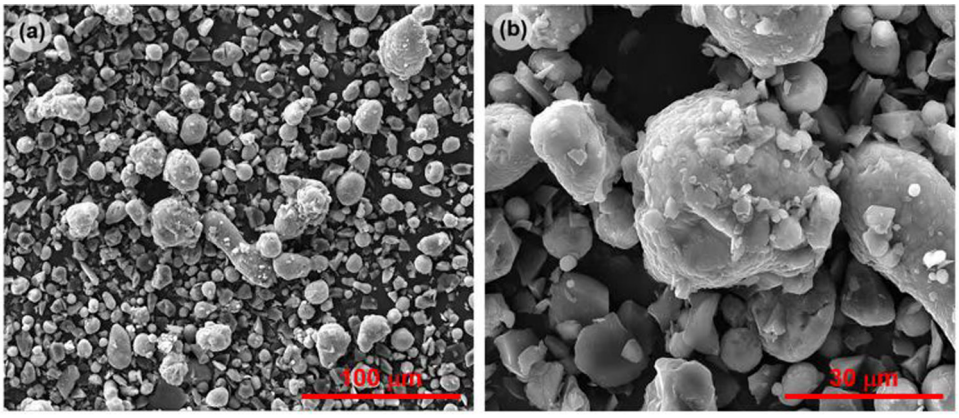

Figure 2: SEM images of mechanically blended B_4C/6061Al powder at low magnification (a) and high magnification (b).

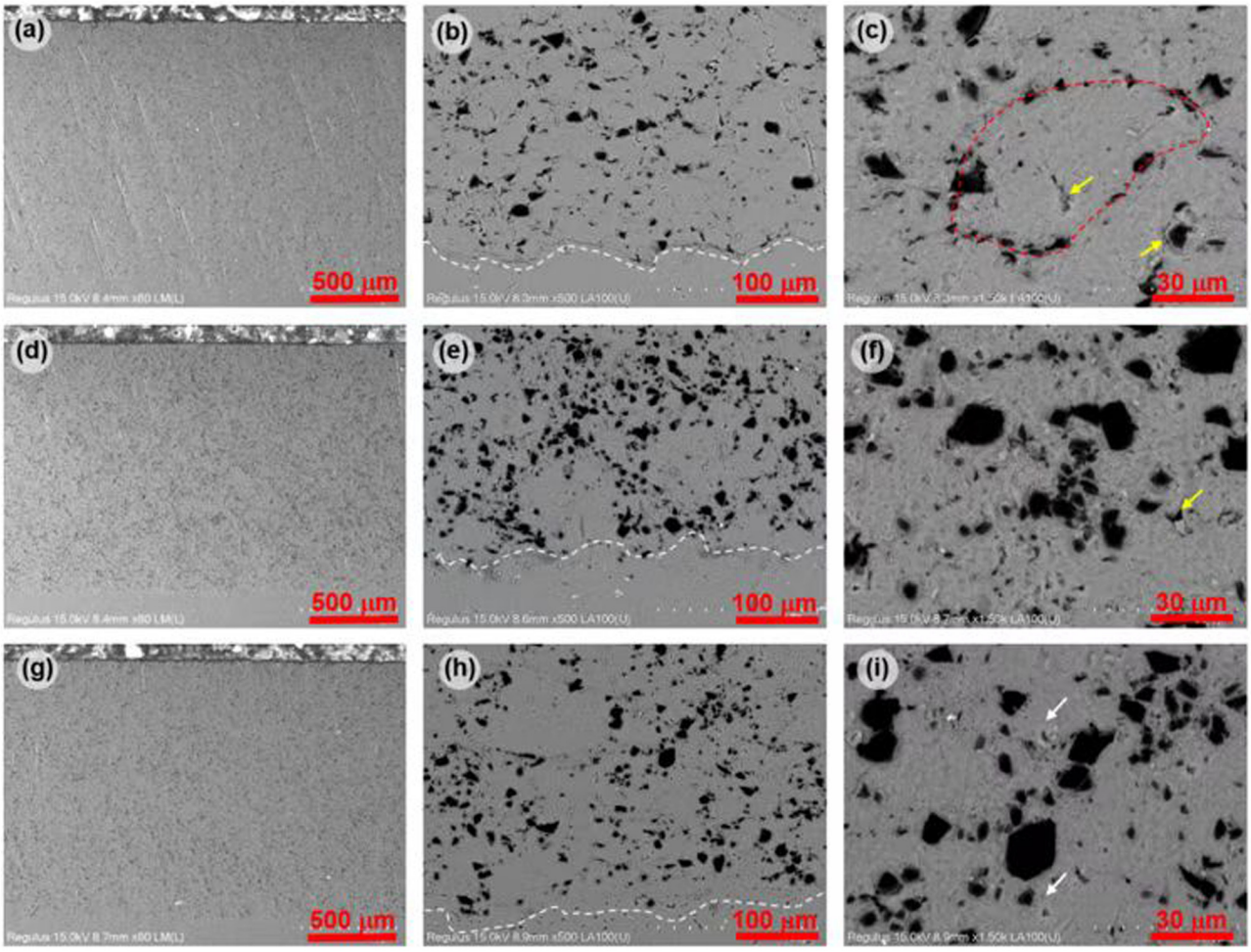

Figure 3: SEM cross-sectional images of as-sprayed (a)–(c), heat-treated (d)–(f) and hot-rolled (g)–(i) samples.

inhomogeneity in the microstructure as well as the resulting properties of the prepared coating. Importantly, the substrate is seriously deformed by the impact of feedstock powders, showing its continuous undulating state, which is considered to be conducive for achieving substrate/coating mechanical interlocking. Further, this highlights the potential of cold spray for repairing/re-manufacturing of unserviceable 6061 Al engineering parts. However, the 6061 Al splat boundaries are clearly visible at the substrate/coating interface, indicating poor substrate/coating interface bonding (Figure 3(b)). When the sample is subjected to the external force, these splat boundaries act as the source for crack generation and propagation which finally result in the spalling of the coating. After heat treatment, the microstructure of the samples is obviously changed (Figure 3(d)–(f)). The morphology of a single 6061Al splat is very difficult to distinguish and the B_4C particles are more evenly distributed throughout the matrix. The content of B_4C particles in the coating significantly increases when compared with that of the as-sprayed sample. This indicates that heat treatment improves the interfacial bonding between 6061Al/6061Al and 6061Al/B_4C particles, and eliminates the work hardening effect in 6061 Al particles. As a result, the plastic flow of 6061 Al particles, during the grinding/polishing process, further limits the separation and pulling of B_4C particles. However, few pores (located at poorly-bonded splat boundaries) are still visible in the coating, as marked by a yellow arrow in Figure 3(f). This suggests that heat treatment has some limitations in improving the microstructure of cold sprayed samples [29]. Second, substrate/coating interface exhibits good bonding state with no defects *i.e.*, splat boundaries. This indicates that heat treatment process promotes the diffusion process between the substrate and the deposited particles and improves the interface bonding. In case of hot rolled sample, the obtained microstructure is almost similar to that of the heat-treated sample. However, the content of B_4C particles is slightly lower than that of the heat-treated sample. This is due to the extremely severe plastic deformation of 6061 Al splats in the rolling process, which induces secondary

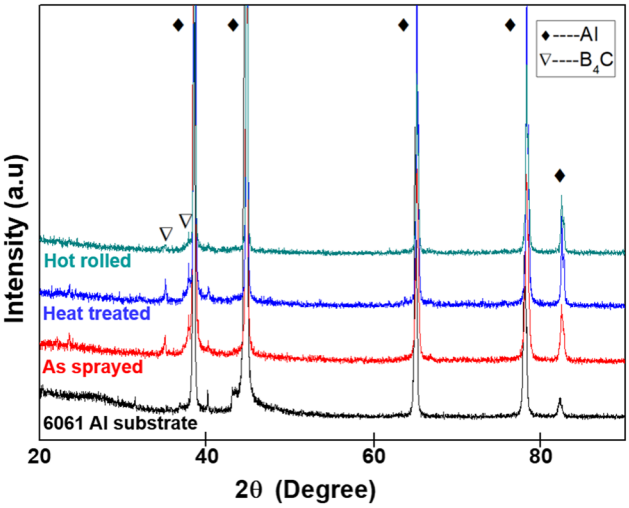

Figure 4: XRD pattern of 6061 Al substrate, as-sprayed, heat-treated and hot-rolled composite coatings.

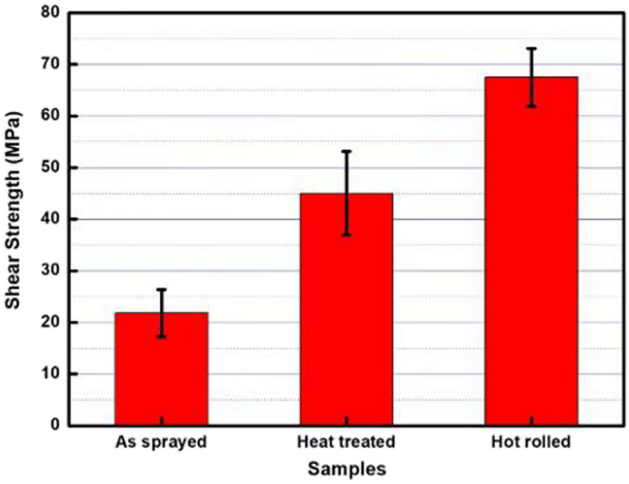

Figure 5: Shear strength values of different coatings.

bonding between B_4C and Al matrix. Consequently, few poorly bonded B_4C particles are pulled out during the grinding process, as marked by white arrow in Figure 3(i).

Figure 4 shows the XRD patterns of as-sprayed, heat treated and hot rolled samples. The Al and B_4C phases can be clearly identified. The intensity of B_4C in XRD pattern is relatively weak due to its low content retained in the coating. Moreover, the diffraction of all the three samples are consistent, indicating there is no new phase formed in heat treatment or rolling process. This is quite consistent with the previous studies on cold spraying of B_4C/Al coatings. Hence, CS is considered to be an excellent deposition technique when compared with other thermal spray processes [30,31].

Figure 5 summarizes the shear strength results, which reflects the bonding strength between the coating and the substrate. The as-sprayed deposit shows the lowest shear strength (21.8 ± 4.5 MPa) at coating/substrate interface among all the three samples. After heat treatment, the bonding state of the coating and the substrate is significantly improved, *i.e.*, the shear strength of coating/substrate is almost doubled (45.0 ± 8.1 MPa). As expected, the hot rolling process results in the highest coating/substrate shear strength (67.5 ± 5.6 MPa) due to sufficient diffusion bonding between the coating and the substrate. The obtained coating/substrate shear strength results seem quite consistent with the interface structure observed in the SEM cross-sectional images shown in Figure 3.

In order to further investigate the effect of heat treatment and hot rolling treatments on the bonding behavior of the coating/substrate, the fractured surface of shear test specimens was examined using SEM, Figure 6. In case of as-sprayed sample, the 6061 Al substrate side shows concave, convex and uneven morphologies, which were caused by the impact of deposited particles during the spraying process, Figure 6(a). It can be clearly observed in the magnified image that B_4C particles are embedded and broken in the concave part of the substrate (as shown by a yellow arrow in Figure 6(b)). In addition, no 6061 Al splat is observed on the substrate. On the composite coating side of the sample, the uneven morphology is also observed. This is attributed to the "pulling off" of some poorly bonded splats during the shearing process, thus resulting in pits at their original position. In addition, a large number of gaps can be observed at the 6061 Al splat boundaries (as indicated by the yellow arrows in Figure 6(d)), indicating poor bonding strength of 6061 Al/6061 Al as well as 6061 Al/B_4C particles in as-sprayed sample. As a result, the particles are easy to be pulled off or shifted to other location under the action of external force. Moreover, the fragmentation of B_4C particles is also observed, which is in line with the cross-sectional backscattered images shown in Figure 3.

For heat treated sample, the surface morphology of the substrate side and the coating side greatly changes after shear tests when compared with the corresponding sides of the as-sprayed sample. It can be observed that the overall surface morphology of the substrate side is relatively flat with some scratches (along the shear direction), while the adhesion of 6061 Al particles is observed on the substrate side. This indicates that the heat treatment can significantly improve the bond strength between the deposited 6061 Al particles and the substrate thereby resisting the external shear force. Moreover, dimple-like structure is quite visible on the surface of the attached 6061 Al splat, as shown in Figure 6(f). This suggests that heat treatment improves the bonding between 6061 Al-6061 Al splats and

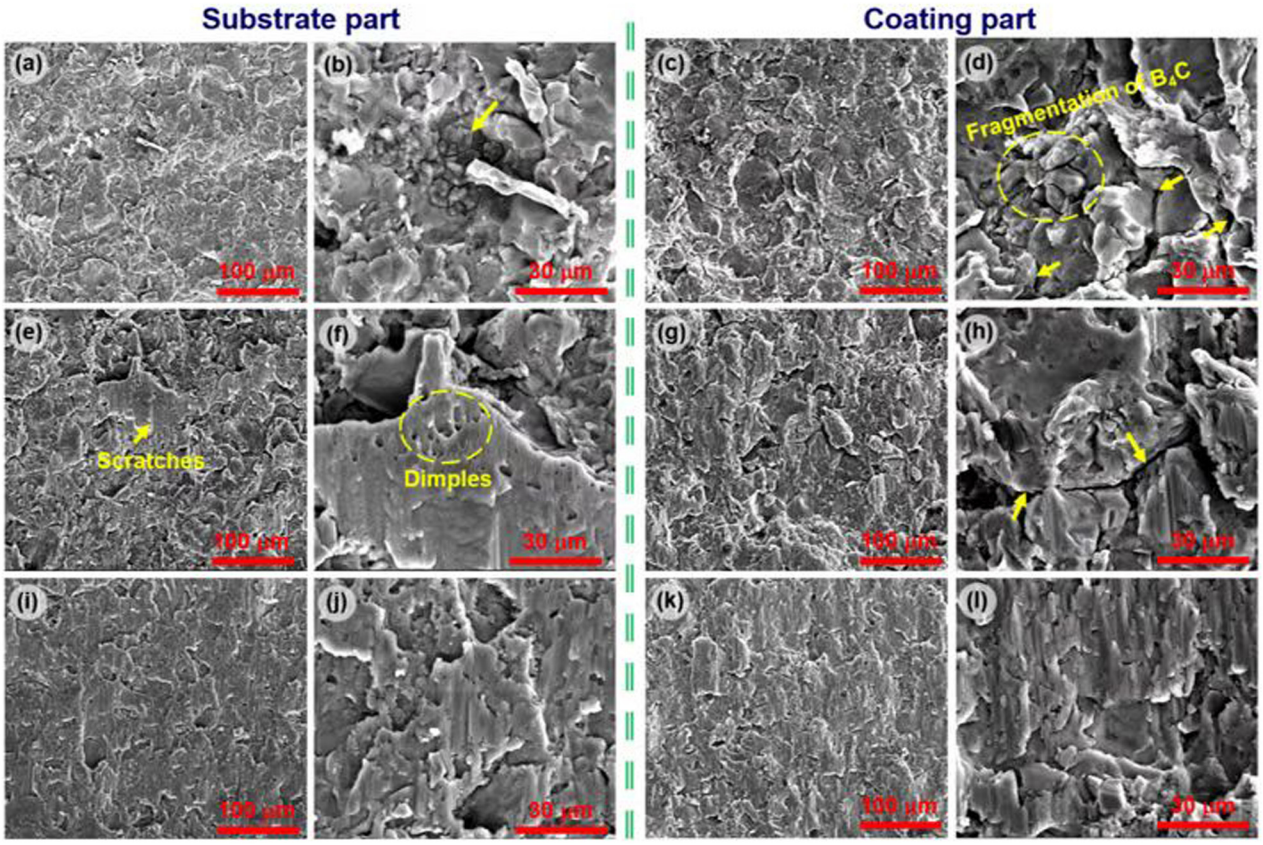

Figure 6: Fracture morphology of different B_4C/6061Al composite coatings after shear tests. (a)–(l) Represents samples with different treatments.

induces plasticity in the sample under external shear force. From the coating side of heat treated sample, it can be seen that the coating surface begins to show the signs of smearing, which also confirms the improved inter-splat bonding. However, the magnified image in Figure 6(h) reveals that there still exist some large-sized cracks at the interface of some splats. This indicates that heat treatment cannot completely heal out the interfaces formed by poorly bonded splats. This is also consistent with the previous study on A380/Al_2O_3 composite coatings [29,32]. The shear surface of the coating and the substrate in hot-rolled sample are much smoother when compared with those of heat treated sample. Moreover, a lot of dimples and smearing marks can be observed, which indicates that the bonding strength and the plasticity of splats are further improved after rolling treatment. During the shearing process, the splats flow adaptively on the uneven surface of the substrate and uniformly cover the substrate surface entirely. On the coating side, it can be observed that the splat boundaries are not obvious and the large-sized gaps are significantly reduced. This indicates that the 6061 Al splat-splat bonding is further improved after the rolling process. The existence of a large number of furrows indicates that B_4C particle could not be adaptively matched with Al particles during the shear process, therefore it was pulled off and moved from its original position.

Hardness results of substrate and coatings under different processing conditions are shown in Figure 7. The

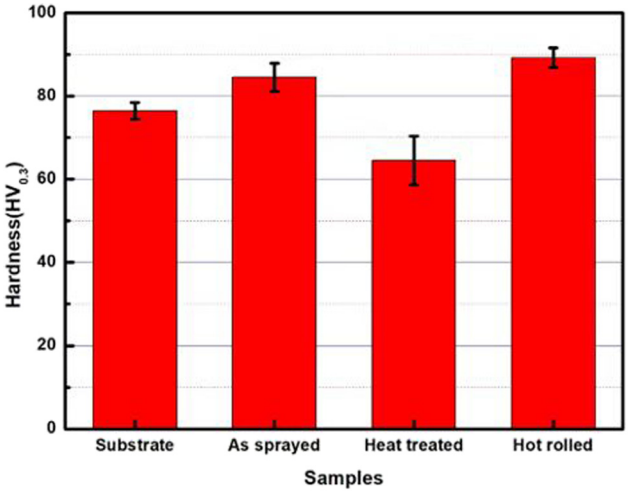

Figure 7: Microhardness of the composite coatings at different processing stages.

hardness of as-sprayed sample is around 82 $HV_{0.3}$, which is only a little higher than that of the substrate. This indicates that low content of B_4C particles and their uneven distribution (along the splat boundary) do not greatly improve the load-bearing capacity of the coating. The hardness of the coating is mainly controlled by the balance between work hardening effect and pore fraction (at the splat boundaries). Quite interestingly, the hardness of heat-treated coating is even much lower than that of 6061 Al substrate. This indicates that the work hardening effect of the coating is eliminated after heat treatment, and the pores at the splat boundaries (which are difficult to be eliminated by heat treatment) become the main reason for reducing the hardness of the material. In contrast, hot-rolled sample shows the highest the hardness value of 89 $HV_{0.3}$. Therefore, hot rolling seems to be an effective technique to efficiently eliminate the pores at splat boundaries thereby improving inter-splat bonding. Moreover, rolling treatment also promotes the uniform distribution of B_4C particles and improves their load bearing capacity in the coating. This may also be the reason for the highest hardness of hot rolled sample.

The wear rates of the substrate and composite coatings under different processing conditions are presented in Figure 8, while Figure 9 shows the corresponding three dimensional (3D) morphologies of wear tracks of the coatings. It can be seen that the as-sprayed 6061 Al/B_4C composite coating on the 6061 Al substrate does not improve its wear resistance. The wear rate of as-sprayed coating is slightly higher than that of the substrate. This can also be confirmed from the 3D wear track morphology, showing smaller width and higher depth when compared with those of the substrate sample. There are two possible

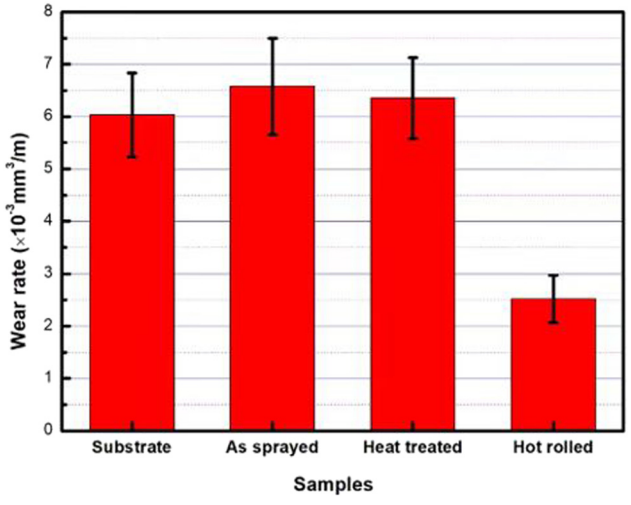

Figure 8: The wear rates of different composite coatings.

reasons for the poor wear resistance of the as-sprayed composite coating: 1) the poorly bonded 6061 Al/6061 Al particles result in the formation of huge amount of defects at the splat boundaries which give rise to the falling off of whole 6061 Al particles during friction; 2) relatively low content of B_4C and its uneven distribution, at the boundaries of large-sized 6061 Al splats, make it difficult to effectively resist the shear force from the counter material and it is much easier for the hard particles to be pulled off from the coating. After heat treatment, the wear rate of the coating ($6.35 \pm 0.78 \times 10^{-3}\,mm^3 \cdot m^{-1}$) is slightly reduced although the hardness value was significantly decreased when compared with that of the as-sprayed coating. This indicates that the increase in hardness, caused by work hardening effect, cannot alone improve the wear resistance of the material [33]. The slight increase in wear resistance after heat treatment may be attributed to the improvement in the bonding state of splats and the decrease in porosity. However, the wear rate of the rolled sample was measured to be $2.51 \pm 0.45 \times 10^{-3}\,mm^3 \cdot m^{-1}$, which is only ~40% of that of the 6061 Al substrate. This provides a new idea for improving the tribological properties of Al alloy plates, *i.e.*, cold spraying (ceramic particle reinforced composite coating) + subsequent hot rolling treatment. From the 3D morphology of the wear track of hot rolled sample, it can be clearly observed that both the width and the depth of the wear track are the smallest among all coatings. In contrary to the smeared wear marks in heat-treated coating, the wear marks of rolled coating show clear furrow like marks. This suggests that after rolling treatment, the structure of the coating becomes very dense. As a result, the deposited particles do not peel off in chunks under the action of shear force. During the rolling process, B_4C particles become uniformly distributed in the coating and act as load bearing phase in the friction process. Consequently, micro-grooves are formed due to the micro-cutting effect of the irregular B_4C particles. Compared with the ploughing effect in heat treated coating, this kind of micro-grooves can significantly reduce the wear loss of the material.

Figure 10 shows representative SEM images of the worn surface of as-sprayed, heat-treated and hot-rolled coatings at different magnifications. For as-sprayed coating, smeared surface and lamellar structure, with brim-like shapes as marked by yellow arrows in Figure 10(c), are observed. This may be attributed to the superior deformation of the outermost coating surface in parallel to the sliding direction. [18,23,34]. This is the typical characteristic of adhesive wear. This situation arises under the action of large adhesion force between the sliding pairs and low stiffness along with high toughness of the material [19]. However, the loose lamellar structure and the existence of large-sized gap in the

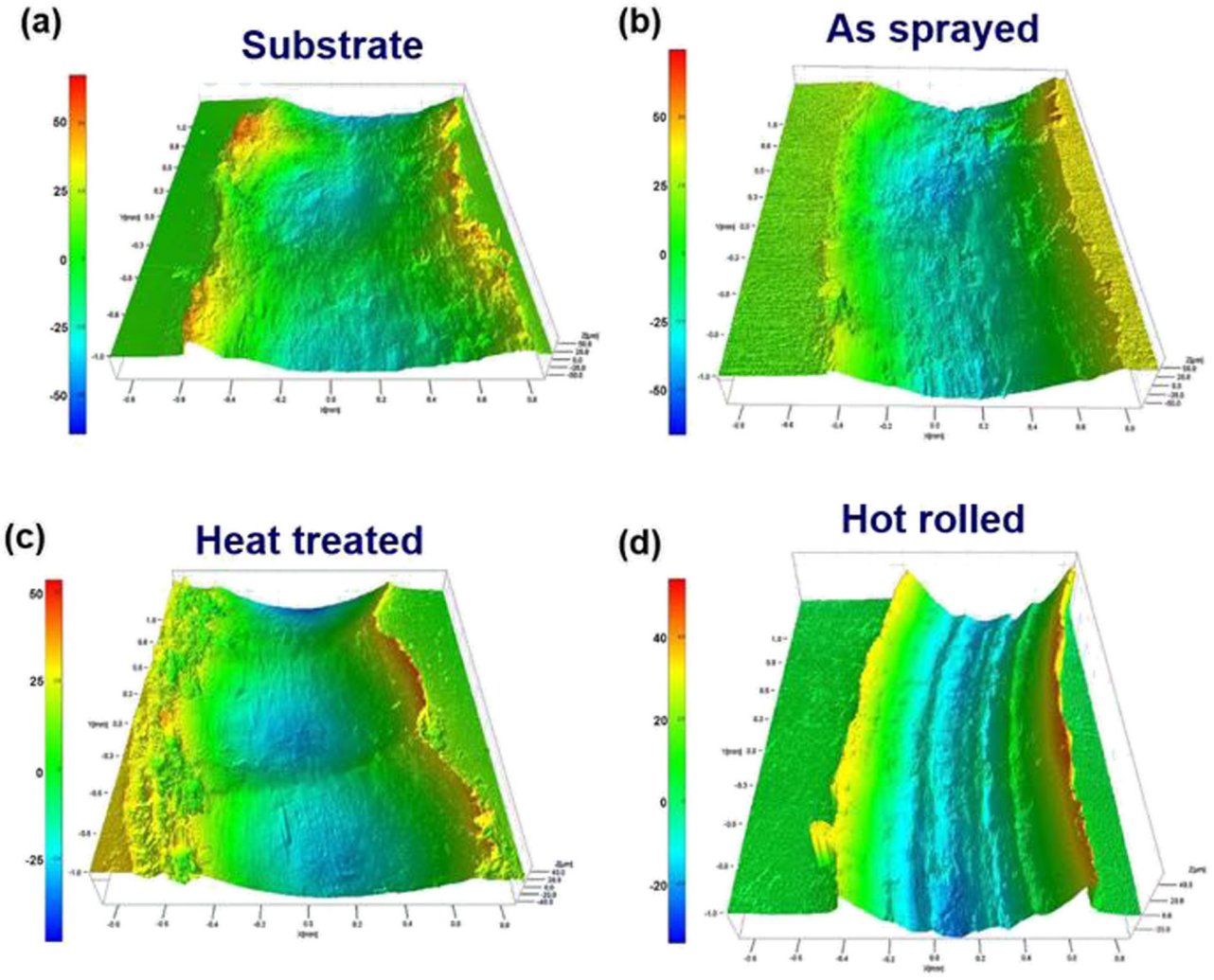

Figure 9: 3D morphologies of wear track of (a) 6061 Al substrate, (b) as-sprayed, (c) heat-treated and (d) hot-rolled composite coatings.

magnified image (Figure 10(c)) indicates the poor bonding between the deposited particles. Moreover, a lot of large sized grooves can be observed, which may be caused by the pulled off B_4C particles as well as the hardened debris formed by repeated plastic deformation (Figure 10(b) and (c)). During friction process, these B_4C particles and debris are easy to be separated from the coating and contribute to a third-body abrasion either alone or in combination with each other, thus accelerating the wear of the coating [35,36]. The wear mechanism of the as-sprayed coating appears to be a combination of adhesive and abrasive wear.

Likewise, the wear track of heat-treated coating also shows evidence of adhesive and abrasive wear, characterized by lamellar smeared surface and micro-grooves, respectively. Compared with the as-sprayed coating (Figure 10(a)–(c)), debris of the heat-treated coating are much denser and smoother, which suggests that heat treatment healed out the splat boundaries and eliminated the work hardening effect in the deposit, (Figure 10(d)–(f)). As a result, the coating exhibits excellent plasticity during sliding friction process. The presence of micro-grooves in Figure 10(e) and (f) indicates that B_4C particles mainly exist within the coating rather than pulled off from the coating. It seems that during the sliding process, B_4C particles moved under the action of shear force, while their sharp angular morphology led to the formation of micro grooves on the surface of wear track. However, it can be observed from the magnified image (Figure 10(f)) that, as a result of repeated sliding operation, the debris progressively became so brittle in nature that it started to peel off from the worn surface, leaving the original pits on the worn surface, as marked by yellow arrows in Figure 10(e). This may result in the high wear rate of the coating and may be attributed to the poorly bonded area in the coating, which could not be healed out by conventional post heat treatment.

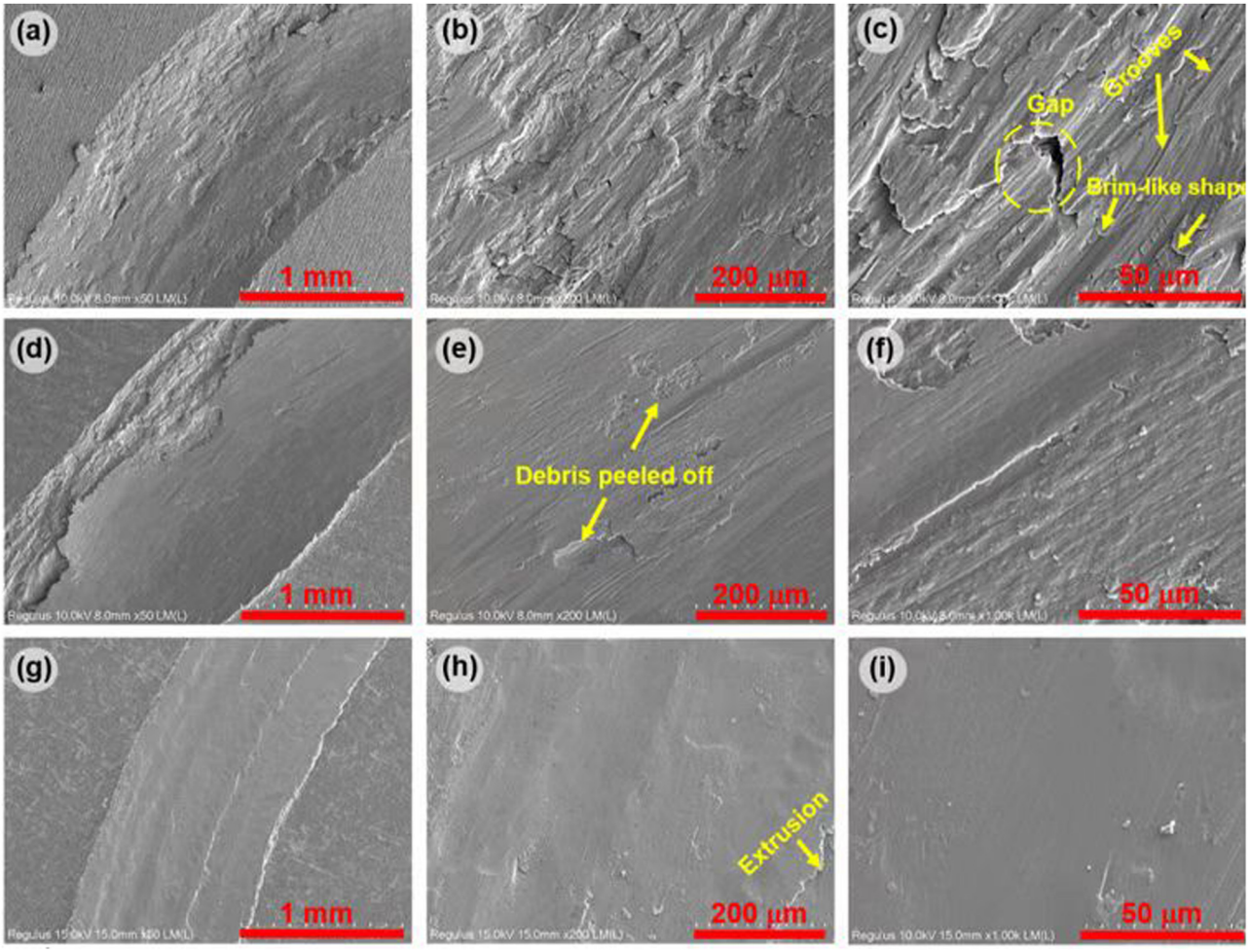

Figure 10: SEM morphologies of wear track of (a)–(c) as-sprayed, (d)–(f) heat-treated and (g)–(i) hot-rolled composite coatings.

The wear surface of hot-rolled sample shows typical adhesive wear, Figure 10(g)–(i). It seems that during the wear process, the 6061 Al particles were plastically deformed (instead of peeling off) under intense shearing and were spread over the wear track layer by layer to form a buffer layer between the coating and the counter alumina ball [37,38]. This buffer layer acted as a lubrication which resulted in the smallest wear loss in hot rolled samples as evident by shallow wear track in Figure 9(d). Further, part of the material is extruded out of the wear track, which is in agreement with the 3D morphology of the wear track shown in Figure 9(d). Moreover, no cracks or delamination of debris is observed, which further confirms that the rolling process has a positive effect on the quality of composite coating. Further, the worn Al_2O_3 counter material was examined to confirm the adhesive wear in rolled sample (results not shown). It was noticed that the counter ball was wrapped with 6061 Al alloy debris which got stuck on its surface gradually and it remained intact throughout the wear test. It is quite interesting to note that very few micro-grooves (formed due to micro-cutting effect by B_4C particles) were formed on the surface of counter ball, which may be attributed to the extremely tight bonding

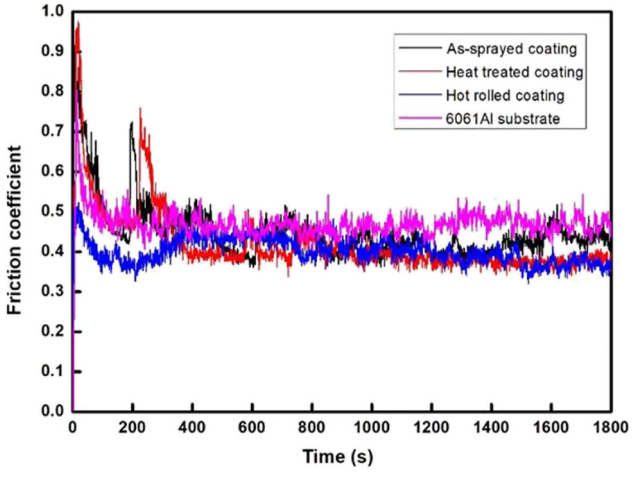

Figure 11: Comparison of friction coefficients of 6061 Al substrate with different B_4C/6061 Al composite coatings.

between B_4C particles and the wrapped 6061 lubricating layer (formed by repeated deformation and extrusion).

The variation in coefficients of friction (COF) with sliding time for the substrate along with different composite coatings is shown in Figure 11. For all the samples, COF shows a fluctuation at the beginning with its value increasing to a peak value and then it stabilizes after the sliding time of ~300 s. It can be observed that the 6061 Al substrate and the as-sprayed composite coating show the higher COF against the Al_2O_3 counter ball (compared with those of heat treated and hot rolled coatings) due to their larger contact area between the ball and the wear track, as shown in Figure 9(a) and (b). Moreover, the COF value for the as-sprayed coating exhibits the largest fluctuation during the friction process, indicating the inhomogeneity in the internal microstructure of the coating. In contrast, the hot rolled and the heat treated coatings show similar COF values against Al_2O_3 counter ball at the stable stage of friction. However, in terms of the whole friction process, the COF value of hot-rolled coating is the most stable, *i.e.*, it experienced the smallest fluctuation during sliding process. This again confirms that the hot rolling post treatment makes the coating structure more compact and uniform. This is quite consistent with the 3D wear morphology and SEM images of the wear track of hot-rolled sample discussed above.

4 Conclusion

For the first time, wear resistance of a 6061 Al alloy plate was improved by depositing B_4C/6061 composite coating using a combination of cold spraying and hot rolling processes. Followings are the main conclusions of this study.

1) As sprayed sample showed local inhomogeneity in the microstructure with B_4C particles generally distributed along 6061 Al splat boundaries. Heat treatment and hot rolling process resulted in the uniform distribution of B_4C particles through efficient healing of the defects and splat boundaries.
2) Heat treatment resulted in two-fold increase in coating/substrate bonding strength when compared with that of the as-sprayed sample. This was attributed to the fact that heat treatment alone cannot completely heal out the poorly bonded interfaces and the residual large sized cracks in the as-sprayed coating.
3) Hot rolling process significantly improved the coating/substrate interface bonding with the two-fold increase in the bonding strength when compared with that of the as-sprayed sample. Fractured surface morphology revealed that the splats exhibit good interfacial bonding and plasticity after hot rolling process.
4) Wear test results showed that the wear resistance of the as-sprayed and the heat-treated composite coatings were even lower than that of the substrate due to the presence of poorly bonded splats and lack of hardness, respectively. In contrast, hot rolling process resulted in much improved tribological properties of the coating with its wear rate only ~40% of that of the substrate.
5) The obtained results show that the presented new idea (*i.e.*, combination of cold spraying and hot rolling treatment) for improving the tribological properties of Al based alloy plates is quite effective. Further, this approach seems equally good for repairing/remanufacturing of unserviceable 6061 Al alloy components.
6) The findings of this work could be considered as a great stride to further extend applications of CS for preparing strong and wear resistant Al alloy plates for automobile and aviation industry.

Acknowledgments: I would like to express my gratitude to all those who helped me during the writing of this Article and IMR Innovation Fund.

Funding information: This work was financially supported by IMR Innovation Fund (No. 2021-PY06).

Author contributions: Tianyu Jiang has written the draft. Naeem ul Haq Tariq helped revise the manuscript. Xiang Qiu analyzed the data and completed the part of the experiments. Qichao Zhang revised the manuscript and provided guidance. Lin Li and Jialun Du provided guidance and funds. All authors have accepted responsibility for the entire content of this manuscript and approved its submission.

Conflict of interest: The authors state no conflict of interest.

Data availability statement: The original contributions presented in the study are included in the article/Supplementary Material, further inquiries can be directed to the corresponding authors.

References

[1] Assadi, H., H. Kreye, F. Gärtner, and T. Klassen. Cold spraying – A materials perspective. *Acta Materialia*, Vol. 116, 2016, pp. 382–407.
[2] Peat, T., A. Galloway, A. Toumpis, P. McNutt, and N. Iqbal. The erosion performance of cold spray deposited metal matrix

composite coatings with subsequent friction stir processing. *Applied Surface Science*, Vol. 396, 2017, pp. 1635–1648.

[3] Yin, S., P. Cavaliere, B. Aldwell, R. Jenkins, H. Liao, W. Li, et al. Cold spray additive manufacturing and repair: Fundamentals and applications. *Additive Manufacturing*, Vol. 21, 2018, pp. 628–650.

[4] Viscusi, A., A. Astarita, L. Carrino, G. D'Avino, C. Nicola, P. Maffettone, et al. Experimental study and numerical investigation of the phenomena occurring during long duration cold spray deposition. *International Review Modelling Simulations*, Vol. 11, No. 2, 2018, pp. 84–92. doi: 10.15866/iremos.v11i2.13619.

[5] Viscusi, A. Numerical investigations on the rebound phenomena and the bonding mechanisms in cold spray processes. *Proceedings of the 21st International ESAFORM Conference on Material Forming, Palermo 23 -25 April 2018. AIP Conf. Proc*, 1960, 100017-1–100017-6. doi: 10.1063/1.5034957.

[6] Bala, N., H. Singh, J. Karthikeyan, and S. Prakash. Cold spray coating process for corrosion protection: a review. *Surface Engineering*, Vol. 30, 2013, pp. 414–421.

[7] Luo, X. T., C. X. Li, F. L. Shang, G. J. Yang, Y. Y. Wang, and C. J. Li. High velocity impact induced microstructure evolution during deposition of cold spray coatings: A review. *Surface and Coatings Technology*, Vol. 254, 2014, pp. 11–20.

[8] Yang, K., W. Li, C. Huang, X. Yang, and Y. Xu. Optimization of cold-sprayed AA2024/Al_2O_3 metal matrix composites via friction stir processing: Effect of rotation speeds. *Journal of Materials Science & Technology*, Vol. 34, 2018, pp. 2167–2177.

[9] Chen, C., S. Gojon, Y. Xie, S. Yin, C. Verdy, Z. Ren, et al. A novel spiral trajectory for damage component recovery with cold spray. *Surface and Coatings Technology*, Vol. 309, 2017, pp. 719–728.

[10] Chen, C., Y. Xie, X. Yan, M. Ahmed, R. Lupoi, J. Wang, et al. Tribological properties of Al/diamond composites produced by cold spray additive manufacturing. *Additive Manufacturing*, Vol. 36, 2020, id. 101434.

[11] Herzog, D., V. Seyda, E. Wycisk, and C. Emmelmann. Additive manufacturing of metals. *Acta Materialia*, Vol. 117, 2016, pp. 371–392.

[12] Meydanoglu, O., B. Jodoin, and E. S. Kayali. Microstructure, mechanical properties and corrosion performance of 7075 Al matrix ceramic particle reinforced composite coatings produced by the cold gas dynamic spraying process. *Surface and Coatings Technology*, Vol. 235, 2013, pp. 108–116.

[13] Kumar, S., S. K. Reddy, and S. V. Joshi. Microstructure and performance of cold sprayed Al-SiC composite coatings with high fraction of particulates. *Surface and Coatings Technology*, Vol. 318, 2017, pp. 62–71.

[14] Cavaliere, P., A. Perrone, and A. Silvello. Mechanical and microstructural behavior of nanocomposites produced via cold spray. *Composite Part. B-Engineering*, Vol. 67, 2014, pp. 326–331.

[15] Xie, X., S. Yin, R. N. Raoelison, C. Chen, C. Verdy, W. Li, et al. Al matrix composites fabricated by solid-state cold spray deposition: A critical review. *Journal of Materials Science & Technology*, Vol. 86, 2021, pp. 20–55.

[16] Irissou, E., J. G. Legoux, B. Arsenault, and C. Moreau. Investigation of Al-Al_2O_3 Cold Spray Coating Formation and Properties. *Journal of Thermal Spray Technology*, Vol. 16, 2007, pp. 661–668.

[17] Qiu, X., N. U. H. Tariq, L. Qi, J. R. Tang, X. Y. Cui, H. Du, et al. Effects of dissimilar alumina particulates on microstructure and properties of cold-sprayed alumina/A380 composite coatings. *Acta Metallurgica Sinica-English*, Vol. 32, 2019, pp. 1449–1458.

[18] Siddique, S., A. A. Bernussi, S. W. Husain, and M. Yasir. Enhancing structural integrity, corrosion resistance and wear properties of Mg alloy by heat treated cold sprayed Al coating. *Surface and Coatings Technology*, Vol. 394, 2020, id. 125882.

[19] Guo, X., G. Zhang, W. Y. Li, L. Dembinski, Y. Gao, H. Liao, et al. Microstructure, microhardness and dry friction behavior of cold-sprayed tin bronze coatings. *Applied Surface Science*, Vol. 254, 2007, pp. 1482–1488.

[20] Li, C. J., X. K. Suo, G. J. Yang, and C. X. Li. Influence of annealing on the microstructure and wear performance of diamond/NiCrAl composite coating deposited through cold spraying. *Materials Science Forum*, Vol. 638–642, 2010, pp. 894–899.

[21] Cheng, R., X. Luo, G. Huang, and C. J. Li. Corrosion and wear resistant WC17Co-TC4 composite coatings with fully dense microstructure enabled by in-situ forging of the large-sized WC17Co particles in cold spray. *Journal of Material Process Technology*, Vol. 296, 2021, id. 117231.

[22] Luo, X. T., Y. K. Wei, Y. Wang, and C. J. Li. Microstructure and mechanical property of Ti and Ti6Al4V prepared by an *in-situ* shot peening assisted cold spraying. *Materials & Design*, Vol. 85, 2015, pp. 527–533.

[23] Qiu, X., N. U. H. Tariq, L. Qi, J. R. Tang, X. Y. Cui, H. Du, et al. Influence of particulate morphology on microstructure and tribological properties of cold sprayed A380/Al_2O_3 composite coatings. *Journal of Materials Science & Technology*, Vol. 44, 2020, pp. 9–18.

[24] Qiu, X., N. U. H. Tariq, J. Q. Wang, J. R. Tang, L. Gyansah, Z. P. Zhao, et al. Microstructure, microhardness and tribological behavior of Al_2O_3 reinforced A380 aluminum alloy composite coatings prepared by cold spray technique. *Surface and Coatings Technology*, Vol. 350, 2018, pp. 391–400.

[25] Zhao, Z., J. Tang, N. U. H. Tariq, H. Liu, Y. Ren, M. Tong, et al. Effect of rolling temperature on microstructure and mechanical properties of Ti/steel clad plates fabricated by cold spraying and hot-rolling. *Materials Science & Engineering, A: Structural Materials: Properties, Microstructure and Processing*, Vol. 795, 2020, id. 139982.

[26] Zhao, Z., N. U. H. Tariq, J. Tang, C. Jia, X. Qiu, Y. Ren, et al. Microstructural evolutions and mechanical characteristics of Ti/steel clad plates fabricated through cold spray additive manufacturing followed by hot-rolling and annealing. *Materials & Design*, Vol. 185, 2020, id. 108249.

[27] Qiu, X., N. U. H. Tariq, L. Qi, Y. N. Zan, Y. J. Wang, J. Q. Wang, et al. *In-situ* Sip/A380 alloy nano/micro composite formation through cold spray additive manufacturing and subsequent hot rolling treatment: Microstructure and mechanical properties. *Journal Alloy Compound*, Vol. 780, 2019, pp. 597–606.

[28] Tariq, N. H., L. Gyansah, J. Q. Wang, X. Qiu, B. Feng, M. T. Siddique, et al. Cold spray additive manufacturing: A viable strategy to fabricate thick B4C/Al composite coatings for neutron shielding applications. *Surface and Coatings Technology*, Vol. 339, 2018, pp. 224–236.

[29] Qiu, X., J. Q. Wang, N. U. H. Tariq, L. Gyansah, J. X. Zhang, and T. Y. Xiong. Effect of heat treatment on microstructure and mechanical properties of A380 aluminum alloy deposited by cold spray. *Journal of Thermal Spray Technology*, Vol. 26, 2017, pp. 1898–1907.

[30] Na, H., G. Bae, S. Shin, S. Kumar, H. Kim, and C. Lee. Advanced deposition characteristics of kinetic sprayed bronze/diamond composite by tailoring feedstock properties. *Composites Science and Technology*, Vol. 69, 2009, pp. 463–468.

[31] Yin, S., Y. Xie, J. Cizek, E. J. Ekoi, T. Hussain, D. P. Dowling, et al. Advanced diamond-reinforced metal matrix composites via cold

spray: Properties and deposition mechanism. *Composite Part. B-Engineering*, Vol. 113, 2017, pp. 44–54.

[32] Qiu, X., N. U. H. Tariq, L. Qi, J. Q. Wang, and T. Y. Xiong. A hybrid approach to improve microstructure and mechanical properties of cold spray additively manufactured A380 aluminum composites. *Materials Science & Engineering, A: Structural Materials: Properties, Microstructure and Processing*, Vol. 772, 2020, id. 138828.

[33] Spencer, K., D. M. Fabijanic, and M. X. Zhang. The use of Al–Al_2O_3 cold spray coatings to improve the surface properties of magnesium alloys. *Surface and CoatingsTechnology*, Vol. 204, 2009, pp. 336–344.

[34] Li, W. Y., G. Zhang, H. L. Liao, and C. Coddet. Characterizations of cold sprayed TiN particle reinforced Al2319 composite coating. *Journal of Material Process Technology*, Vol. 202, 2008, pp. 508–513.

[35] Shockley, J. M., S. Descartes, P. Vo, E. Irissou, and R. R. Chromik. The influence of Al_2O_3 particle morphology on the coating formation and dry sliding wear behavior of cold sprayed Al–Al_2O_3 composites. *Surface and Coatings Technology*, Vol. 270, 2015, pp. 324–333.

[36] Yandouzi, M., A. J. Böttger, R. W. A. Hendrikx, M. Brochu, P. Richer, A. Charest, et al. Microstructure and mechanical properties of B4C reinforced Al-based matrix composite coatings deposited by CGDS and PGDS processes. *Surface and Coatings Technology*, Vol. 205, 2010, pp. 2234–2246.

[37] Triantou, K. I., D. I. Pantelis, V. Guipont, and M. Jeandin. Microstructure and tribological behavior of copper and composite copper + alumina cold sprayed coatings for various alumina contents. *Wear*, Vol. 336–337, 2015, pp. 96–107.

[38] Yin, Z., S. Tao, X. Zhou, and C. Ding. Tribological properties of plasma sprayed Al/Al_2O_3 composite coatings. *Wear*, Vol. 263, 2007, pp. 1430–1437.